Dispersion error reduction of absorption finite elements based on equivalent fluid model

Okuzono, Takeshi

Sakagami, Kimihiro

ACOUSTICAL LETTER

Dispersion error reduction of absorption finite elements based on equivalent fluid model

Takeshi Okuzono* and Kimihiro Sakagami

Environmental Acoustic Laboratory, Department of Architecture, Graduate School of Engineering, Kobe University, 1–1 Rokkodai, Nada, Kobe, 657–8501 Japan

(*Received 6 March 2018, Accepted for publication 5 April 2018*)

Keywords: FEM, Discretization error, Porous material, Sound absorber
PACS number: 43.55.Ka, 43.55.Dt, 43.55.Ev [doi:10.1250/ast.39.362]

1. Introduction

This paper describes reduction of the dispersion error of absorption finite elements (FEs) based on an equivalent fluid model, which has been used widely to model porous sound absorbers in the acoustic finite element method (FEM) [1–7]. In absorption FEs, the air in a rigid porous medium is modeled at a macroscopic scale as an equivalent fluid with a complex effective density and a complex bulk modulus. The model incorporates consideration of the dissipative effects of viscosity and heat conduction. In doing so, sound propagation in a rigid porous medium is described by a Helmholtz equation with a complex wavenumber.

Acoustic finite element analysis governed by Helmholtz equation is well known to have inherent discretization error, called dispersion error, which is defined as the difference between the exact wavenumber and the numerical wavenumber. Because of that error, the spatial discretization requirement, known as a rule of thumb, is imposed to yield reliable results. The dispersion error can be reduced by increasing mesh resolution, but the strategy is computationally expensive for large-scale problems such as analyses in spatially large domains. Several methods that been well reviewed in the literature have been designed to achieve efficient analyses by reducing the dispersion error [8]. For reducing the dispersion error of absorption FEs based on an equivalent fluid model, the present paper uses a simple dispersion reduction method called modified integration rules (MIR) [9].

MIR reduces the dispersion error by simply changing the numerical integration points of element stiffness and mass matrices from conventional integration points, without additional computational cost. The modified integration points are derived using dispersion error analysis to minimize the dispersion error. Some reports have described the effectiveness of MIR for wave propagation problems with real wavenumbers [9–11]. However, the applicability of MIR to absorption FEs based on an equivalent fluid model that discretizes the Helmholtz equation with complex wavenumber remains unclear.

This paper first presents that the dispersion error of eight-node hexahedral absorption FEs is reduced by the same MIR as in the case of real wavenumber. Then two basic plane wave propagation problems in a porous domain and coupled air-porous domain demonstrate the effectiveness of absorption FEs using MIR.

2. Theory

2.1. Absorption FEs based on an equivalent fluid model

Sound propagation in isotropic porous media Ω_p (complex effective density: ρ_e, complex bulk modulus: K_e) with a rigid frame is described by the following Helmholtz equation with complex wavenumber k_e as

$$\nabla^2 p + k_e^2 p = 0, \tag{1}$$

where p represents the sound pressure. The FE discretization of the weak form of Eq. (1) engenders the following system of linear equations

$$\left[\boldsymbol{K}_p - k_e^2 \boldsymbol{M}_p + ik_0\left(\frac{\rho_e}{\rho_0}\right)\boldsymbol{C}_p\right]\boldsymbol{p} = i\omega\rho_e v_p \boldsymbol{W}, \tag{2}$$

with rigid, vibration, and impedance boundary conditions. As shown above, $\boldsymbol{K}_p$, $\boldsymbol{M}_p$, $\boldsymbol{C}_p$ respectively represent the stiffness, mass, and dissipation matrices. Vectors $\boldsymbol{p}$ and $\boldsymbol{W}$ are the sound pressure vector and distribution vector. Furthermore, i, ρ_0, ω, and v_p respectively denote the imaginary unit, air density, angular frequency, particle velocity at the boundary of Ω_p. In the use of the equivalent fluid model, the quantities of complex effective density ρ_e and complex bulk modulus K_e of equivalent fluid (or complex wavenumber k_e and characteristic impedance Z_c) are necessary. These quantities are obtained from empirical models such as the Miki model [12] and semi-phenomenological models such as the JCA model [13]. The present analyses use the Miki model [12] to calculate the k_e and Z_c of porous material.

2.2. Coupling of air-porous domains

Sound propagation in air domain Ω_0 (air density, ρ_0; bulk modulus, K_0) is described using the following Helmholtz equation with real wavenumber k_0 as

$$\nabla^2 p + k_0^2 p = 0. \tag{3}$$

The FE discretization of the equation above with rigid, vibration, and impedance boundary conditions engenders a linear system of equations for Ω_0:

$$[\boldsymbol{K}_0 - k_0^2 \boldsymbol{M}_0 + ik_0 \boldsymbol{C}_0]\boldsymbol{p} = i\omega\rho_0 v_0 \boldsymbol{W}, \tag{4}$$

where $\boldsymbol{K}_0$, $\boldsymbol{M}_0$, and $\boldsymbol{C}_0$ respectively denote the stiffness, mass,

*e-mail: okuzono@port.kobe-u.ac.jp

and dissipation matrices in terms of Ω_0. Furthermore, v_0 is the particle velocity at the boundary of Ω_0. The air domain Ω_0 and porous domain Ω_p are coupled by the continuity condition of sound pressure and particle velocity at the interface of both domains. The coupled linear system of equations is expressed as

$$[(\boldsymbol{K}_0 - k_0^2\boldsymbol{M}_0 + ik_0\boldsymbol{C}_0) + (\varepsilon\boldsymbol{K}_\mathrm{p} - \varepsilon k_\mathrm{e}^2\boldsymbol{M}_\mathrm{p} + ik_0\boldsymbol{C}_\mathrm{p})]\boldsymbol{p} = i\omega\rho_0 v\boldsymbol{W}, \quad (5)$$

with parameter $\varepsilon = \rho_0/\rho_\mathrm{e}$. The value v is the particle velocity of boundary surfaces.

2.3. Modified integration rules

For the eight-node hexahedral FEs the Gauss–Legendre rules with two integration points in each direction are commonly used to calculate the element stiffness and mass matrices. The integration points are given as

$$\alpha_k = \alpha_m = \pm\sqrt{1/3}, \quad (6)$$

where α_k and α_m respectively denote the integration points of element stiffness and mass matrices. Instead of Eq. (6), MIR uses the following modified integration points [9] derived from dispersion error analysis as

$$\alpha_k = \alpha_m = \pm\sqrt{2/3}. \quad (7)$$

As described previously, the effectiveness of MIR for wave propagation problems with real wavenumber has been demonstrated in earlier papers [9,11]. Nevertheless, the applicability for the problems with complex wavenumber has not been discussed.

3. Dispersion error analysis

The dispersion error is defined as the relative error between exact complex wavenumber k_e and numerical complex wavenumber $\tilde{k}_\mathrm{e}$. In a spherical coordinate system, the solution is a plane wave of the form $\exp[ik_\mathrm{e}(x\sin\theta\cos\phi + y\sin\theta\sin\phi + z\cos\theta)]$, where θ and ϕ respectively denote the azimuth and elevation. The approximate solution of the plane wave is given as

$$\tilde{p}_{x,y,z} = \exp[i\tilde{k}_\mathrm{e}(x\sin\theta\cos\phi + y\sin\theta\sin\phi + z\cos\theta)]. \quad (8)$$

Hereinafter, we consider plane wave propagation in infinite porous media, discretizing uniformly by rectangular eight-node hexahedral FEs of size $d_x \times d_y \times d_z$. In the actual evaluation of dispersion error, only a region that consists of eight elements is examined here, as shown in Fig. 1. The dispersion error can be evaluated by constructing the FE equation of Eq. (2) at the center node (x, y, z). Then substituting the approximate plane wave solution of Eq. (8) into the FE equation engenders the following dispersion relation between k_e and $\tilde{k}_\mathrm{e}$ as

$$k_\mathrm{e} = \frac{2}{d_x d_y d_z} \times \sqrt{\frac{C'_x B_y B_z d_y^2 d_z^2 + C'_z B_x B_y d_x^2 d_y^2 + C'_y B_z B_x d_z^2 d_x^2}{A_x A_y A_z}}, \quad (9)$$

with

$$A_x = \alpha_k^2 C_x - \alpha_k^2 - 1 - C_x, \quad A_y = \alpha_k^2 C_y - \alpha_k^2 - 1 - C_y,$$

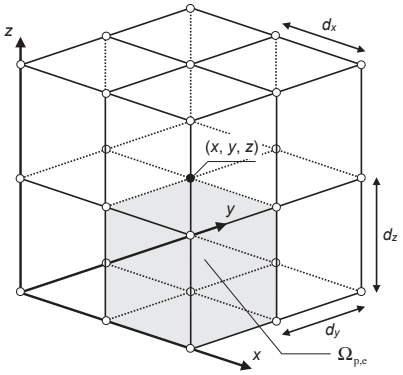

Fig. 1 27 node 8 element patch for dispersion error analysis: $\Omega_{\mathrm{p,e}}$ represents an absorption element.

$$A_z = \alpha_k^2 C_z - \alpha_k^2 - 1 - C_z, \quad B_x = \alpha_m^2 C_x - \alpha_m^2 - 1 - C_x,$$
$$B_y = \alpha_m^2 C_y - \alpha_m^2 - 1 - C_y, \quad B_z = \alpha_m^2 C_z - \alpha_m^2 - 1 - C_z,$$
$$C'_x = C_x - 1, \quad C'_y = C_y - 1, \quad C'_z = C_z - 1, \quad (10)$$

and

$$C_x = \cos(\tilde{k}_\mathrm{e} d_x \sin\theta\cos\phi), \quad C_y = \cos(\tilde{k}_\mathrm{e} d_y \sin\theta\sin\phi),$$
$$C_z = \cos(\tilde{k}_\mathrm{e} d_z \cos\theta). \quad (11)$$

Taking Taylor expansion of k_e in terms of $\tilde{k}_\mathrm{e}$, the dispersion error for conventional integration points of Eq. (6) can be expressed approximately as

$$\frac{k_\mathrm{e} - \tilde{k}_\mathrm{e}}{k_\mathrm{e}} \approx \frac{k_\mathrm{e}^2}{24}(d_x^2\sin^4\theta\cos^4\phi + d_y^2\sin^4\theta\sin^4\phi + d_z^2\cos^4\theta). \quad (12)$$

The conventional eight-node hexahedral absorption FEs have second-order accuracy in terms of dispersion error. However, the dispersion error with modified integration points of Eq. (7) is given approximately as

$$\frac{k_\mathrm{e} - \tilde{k}_\mathrm{e}}{k_\mathrm{e}} \approx \frac{-k_\mathrm{e}^4}{480}(d_x^4\sin^6\theta\cos^6\phi + d_y^4\sin^6\theta\sin^6\phi + d_z^4\cos^6\theta). \quad (13)$$

The absorption FEs with MIR have fourth-order accuracy. The MIR reduces the dispersion error even for a Helmholtz equation with a complex wavenumber.

4. Numerical experiments

The performance of absorption FEs with MIR was tested using two plane wave propagation problems: plane wave propagation in a porous domain and plane wave propagation in an air–porous domain. We also use conventional air and absorption FEs for comparison.

4.1. Plane wave propagation in a porous domain

We consider plane wave propagation in porous domain Ω_p (the flow resistivity of medium $R = 5{,}000, 10{,}000, 20{,}000$ $\mathrm{N\,s/m^4}$) with vibration boundary Γ_v ($v_\mathrm{p} = 1\,\mathrm{m/s}$) and rigid boundary Γ_0, as presented in Fig. 2(a). The sound pressure was calculated, respectively, at 1 kHz, 1.5 kHz, 2 kHz, 2.5 kHz, and 3 kHz. Cubic elements with the length of 0.025 m were used for spatial discretization. The theoretical sound pressure p_p at point x is calculated using superposition

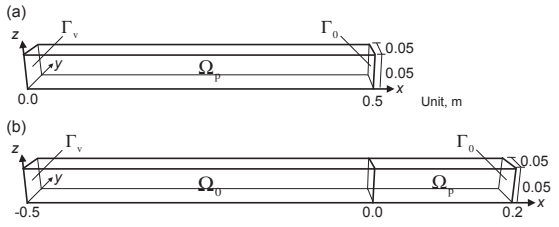

Fig. 2 Plane wave propagation problems in (a) a porous domain and (b) air–porous domain.

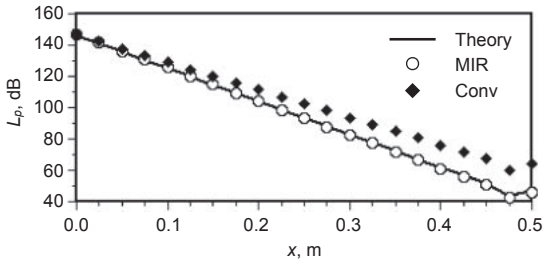

Fig. 3 L_p at 2 kHz among theory, FEM with absorption FEs using MIR (MIR), and FEM with conventional absorption FEs (Conv).

of two plane waves propagating toward the positive and negative abscissas,

$$p_{\mathrm{p}}(x) = Ae^{-ik_{\mathrm{e}}x} + A'e^{ik_{\mathrm{e}}x}, \tag{14}$$

with the following boundary conditions:

$$\frac{\partial p_{\mathrm{p}}(0)}{\partial n} = -i\omega\rho_{\mathrm{e}}v_{\mathrm{p}}, \quad \frac{\partial p_{\mathrm{p}}(0.5)}{\partial n} = 0. \tag{15}$$

Figure 3 presents a comparison of sound pressure level (L_p) at 2 kHz among theory, FEM with the absorption FEs using MIR and FEM with conventional absorption FEs for the case of $R = 20{,}000\,\mathrm{N\,s/m^4}$. The present FEs with MIR agree well with theory. Conventional FEs tend to underestimate dissipation for longer propagation distance. Although the result is omitted, the present FEs with MIR tend to overestimate the dissipation for longer propagation distance at higher frequencies. The results are the same as those obtained in cases with other flow resistivity values. Figure 4 shows the relative error norm e_{L} of L_p in terms of location x in Ω_{p} calculated as

$$e_{\mathrm{L}} = \frac{\|L_p - \tilde{L}_p\|_2}{\|L_p\|_2}, \tag{16}$$

where L_p and $\tilde{L}_p$ respectively represent the theoretical and numerical values. The present FEs with MIR are more accurate than the conventional FEs in all cases. The present FEs show nearly equal error up to 2 kHz independent of the flow resistivity values. At higher frequencies, the error increases for larger flow resistivity, but the magnitude is smaller than that of the conventional FEs.

4.2. Plane wave propagation in air–porous domain

We consider a plane wave propagation in air Ω_0–porous domain Ω_{p} ($R = 5{,}000, 10{,}000\,\mathrm{N\,s/m^4}$) with vibration boun-

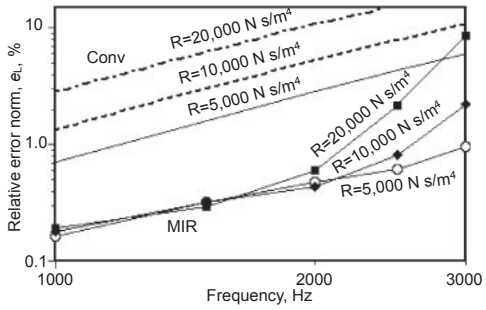

Fig. 4 Relative error norm e_{L} of FEM with absorption FEs using MIR (MIR), and FEM with conventional absorption FEs (Conv) for the case with $R = 5{,}000$, 10,000, and $20{,}000\,\mathrm{N\,s/m^4}$.

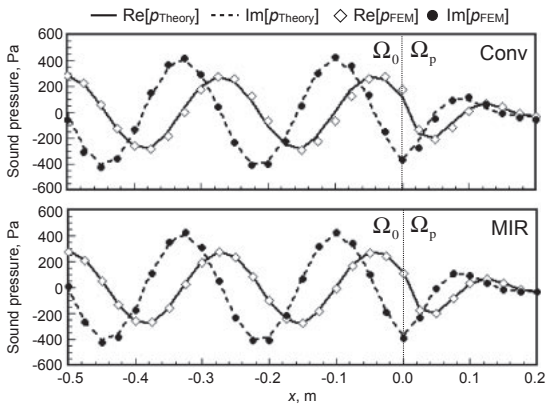

Fig. 5 Complex sound pressure at 1.5 kHz of theory, FEM with absorption FEs using MIR (MIR), and FEM with conventional absorption FEs (Conv) for the case with $R = 10{,}000\,\mathrm{N\,s/m^4}$.

dary Γ_{v} ($v_0 = 1\,\mathrm{m/s}$) and rigid boundary Γ_0, as presented in Fig. 2(b). The sound pressure was calculated, respectively, at 1 kHz, 1.5 kHz, 2 kHz and 2.5 kHz. Element size is the same as that given in the previous section. The theoretical sound pressure at point x is given as

$$\begin{aligned} p_0(x) &= Ae^{-ik_0x} + A'e^{ik_0x} \quad (-0.5 \le x \le 0), \\ p_{\mathrm{p}}(x) &= Be^{-ik_{\mathrm{e}}x} + B'e^{ik_{\mathrm{e}}x} \quad (0 \le x \le 0.2), \end{aligned} \tag{17}$$

with the following boundary conditions of

$$\begin{aligned} &\frac{\partial p_0(-0.5)}{\partial n} = -i\omega\rho_0 v_0, \quad \frac{\partial p_{\mathrm{p}}(0.2)}{\partial n} = 0, \\ &-\frac{1}{i\omega\rho_0}\frac{\partial p_0(0)}{\partial n} = -\frac{1}{i\omega\rho_{\mathrm{e}}}\frac{\partial p_{\mathrm{p}}(0)}{\partial n}, \quad p_0(0) = p_{\mathrm{p}}(0), \end{aligned} \tag{18}$$

where p_0 denotes the sound pressure in Ω_0.

Figures 5 and 6 present complex sound pressure at 1.5 kHz and 2.5 kHz among theory, FEM with MIR in both air and porous domains, and conventional FEM without MIR in both domains, for the case of $R = 10{,}000\,\mathrm{N\,s/m^4}$. Both the present FEM with MIR and conventional FEM show good agreement with theory at 1.5 kHz. However, detailed observations show that the conventional FEM has slightly longer wavelength with increasing distance x. This results from the

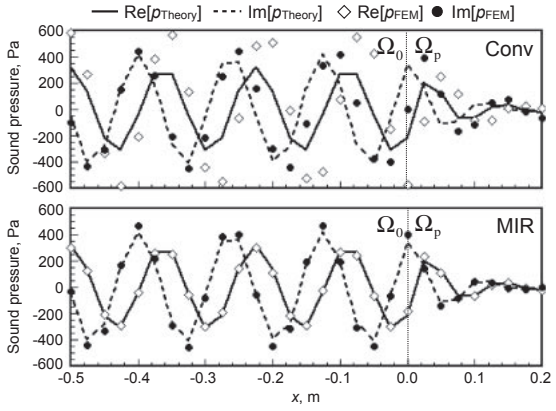

Fig. 6 Complex sound pressure at 2.5 kHz of theory, FEM with absorption FEs using MIR (MIR), and FEM with conventional absorption FEs (Conv) for the case with $R = 10{,}000\,\mathrm{N\,s/m^4}$.

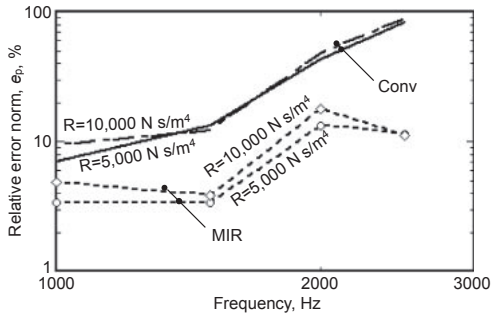

Fig. 7 Relative error norm e_p of FEM using MIR (MIR), and conventional FEM (Conv) for the case with $R = 5{,}000$ and $10{,}000\,\mathrm{N\,s/m^4}$.

slight increase of numerical sound speed, as expected from Eq. (12). At 2.5 kHz, the present FEM shows much better agreement than the conventional FEM. The conventional method shows marked discrepancy because of the larger dispersion error. We measured the relative error norm e_p of complex sound pressure in terms of location x, which is defined as

$$e_\mathrm{p} = \frac{\|p - \tilde{p}\|_2}{\|p\|_2}, \tag{19}$$

where p and $\tilde{p}$ respectively denote theoretical and numerical complex sound pressure. Figure 7 presents the results. It is clear that the present FEM with MIR exhibits lower error in all cases.

5. Conclusions

Dispersion error analysis showed that the eight-node hexahedral absorption FEs based on equivalent fluid model has fourth-order accuracy in terms of dispersion error using the same MIR, as in the case of a real wavenumber. Furthermore, the two basic plane wave propagation problems confirmed that absorption FEs using MIR show better accuracy than conventional FEs, even in coupled analysis of air–porous domains. More detailed error analyses under various conditions remain as subjects of future research.

References

[1] A. Craggs, "A finite element model for rigid porous absorbing materials," *J. Sound Vib.*, **61**(1), 101–111 (1978).
[2] A. Craggs, "Coupling of finite element acoustic absorption models," *J. Sound Vib.*, **66**, 605–613 (1979).
[3] V. Easwaran and M. L. Munjal, "Finite element analysis of wedges used in anechoic chambers," *J. Sound Vib.*, **160**, 333–350 (1993).
[4] T. Sakuma, T. Iwase and M. Yasuoka, "Prediction of sound fields in rooms with membrane materials: Development of a limp membrane element in acoustical FEM analysis and its application," *J. Archit. Plann. Environ. Eng.*, **505**, 1–8 (1998).
[5] W. H. Chen, F. C. Lee and D. M. Chiang, "On the acoustic absorption of porous materials with different surface shapes and perforated plates," *J. Sound Vib.*, **237**, 337–355 (2000).
[6] R. Tomiku and T. Otsuru, "Sound fields analysis in an irregular-shaped reverberation room by finite element method," *J. Archit. Plann. Environ. Eng.*, **551**, 9–15 (2002) (in Japanese).
[7] M. Aretz and M. Vorländer, "Efficient modeling of absorbing boundaries in room acoustic FE simulations," *Acta Acust. united Ac.*, **96**, 1042–1050 (2010).
[8] L. L. Thompson, "A review of finite-element methods for time-harmonic acoustics," *J. Acoust. Soc. Am.*, **119**, 1315–1330 (2006).
[9] M. N. Guddati and B. Yue, "Modified integration rules for reducing dispersion error in finite element methods," *Comput. Methods Appl. Mech. Eng.*, **193**, 275–287 (2004).
[10] T. Okuzono, T. Otsuru, R. Tomiku and N. Okamoto, "A finite-element method using dispersion reduced spline elements for room acoustics simulation," *Appl. Acoust.*, **79**, 1–8 (2014).
[11] T. Okuzono and K. Sakagami, "A frequency domain finite element solver for acoustic simulations of 3D rooms with microperforated panel absorbers," *Appl. Acoust.*, **129**, 1–12 (2018).
[12] Y. Miki, "Acoustical properties of porous materials — Modifications of Delany-Bazley models —," *J. Acoust. Soc. Jpn.* (*E*), **11**, 19–24 (1990).
[13] J. F. Allard and N. Atalla, "Sound propagation in porous materials having a rigid frame," in *Propagation of Sound in Porous Media: Modeling Sound Absorbing Materials*, 2nd ed. (John Wiley & Sons, Chichester, 2009), Chap. 5, pp. 73–109.